Studies of Spatial and Temporal Surface Current Turbulence outside Golden Gate

Donald Barrick and William Rector
1914 Plymouth Street
CODAR Ocean Sensors, Ltd.
Mountain View, CA 94043 USA
don@codar.com

***Abstract*—This contribution examines the zero-mean random variability of surface currents seen by drifters and HF radar outside of Golden Gate in the Pacific. Seeding multiple drifters within cells of radar spatial and temporal scale sizes allows an understanding of this natural variability. Using the drifter velocity standard deviations to establish these turbulent motions is important in assessing radar errors, as it allows apportioning the differences between natural surface motions (that may not be of interest in studying mean flows) and radar noise. Numbers obtained in this study are about 4.1 cm/s for spatial and 1.2 cm/s for temporal drifter standard deviations, respectively. Similar numbers for radar standard deviations are 8.2 and 3.2 cm/s. RMS differences between radar and drifter radial velocities here are typically 8-9 cm/s.**

Keywords-component; HF radar; surface currents; upper-layer turbulence

I. INTRODUCTION

As soon as the first measurements of surface currents with coastal HF radars began in the early 1970s, attempts were made to assess their accuracy [1, 2, 3]. This was done by comparing with other sensors that measured velocity near the surface, such as drifters, ADCPs, or moored current meters. The usual methods included examining RMS differences, scatter plots, and correlation coefficients between the radar and other sensor. Often differences were assumed to be radar error, as the other sensor was taken to be "truth." Although it was recognized early on that the disparate nature of the two measurements could account for some of the differences (rather than radar errors), it was not until 1997 that the first look at apportioning errors was undertaken [4].

Consider the above metrics in light of differences, which can be of two types: biases (mean differences) and zero-mean random statistical fluctuations. The first metric which is often calculated in comparisons is RMS differences; it includes both types of differences, i.e., mean and random fluctuations. Scatter plots also reveal biases/means as well as random fluctuations; i.e., the slope of the regression line is a measure of the bias and the scatter about this line depends on the random fluctuations. Correlation coefficients, on the other hand, depend predominantly on the random fluctuations between sensors, and most often conceal biases. As an example of the latter, consider two measurements of a sinusoidal (tidal) flow with no random differences, but one is biased and sees one half the amplitude swing as the other. The correlation coefficient will be 100%, but the RMS difference will be unacceptably large.

As a single ungraphed number, therefore, the RMS difference is a preferred comparison metric. Suppose the bias/mean term of this difference is zero. Is the remaining non-zero RMS value a measure of radar error? The first study to answer this occurred in 2006 by Rutgers University [5]. Two ADCPs deployed within a single long-range SeaSonde radar cell observed raw RMS radial velocity component differences that were the same as radar-to-ADCP differences -- 6-7 cm/s (with essentially zero mean bias). RMS differences for the tidally filtered radial components, however, dropped to 1-2 cm/s for both ADCP/ADCP and ADCP/radar, another suggestion of negligible instrument bias in this case. This demonstrated that natural variability -- or turbulence -- of the raw surface currents played a significant role in RMS difference measurements. It suggests that even with no bias, the remaining RMS difference was not due to radar (or ADCP) error. Sub-grid-scale variability is the cause of the RMS differences seen here. Thus it became obvious that this should be measured and taken into account when trying to assess radar measurement error.

A significant advance toward measuring subgrid-scale variability and relating it to RMS differences seen in radar/drifter comparisons was the use of many drifters within the same radar cell pioneered by Ohlmann et al. [6], where the drifters are constantly reseeded so that several are observed simultaneously within a defined radar/area cell. That work summarized the statistics (RMS differences, mean differences, correlation coefficients, scatter plots). Drifter velocities were resolved into components radial to various radars (called radials). These revealed radial standard deviations of 2 - 3 cm/s within 2 x 2 km square cells averaged over an hour, and maximum drifter spans within these cells up to 10 cm/s. Drifter-to-radar RMS differences were perhaps 50% greater, with one or two cases where differences were as high as 12 cm/s. These statistical summary tables and graphs did not reveal how much of the variability was spatial or temporal. Both individual radar and drifter measurements were averaged, outputted, and compared over hourly intervals.

In the next section, we discuss a 4-day drifter deployment test done West of Golden Gate off California that we analyze in this paper. Next we discuss the measurements and processing done by the radar to calculate radial surface velocities. We start our analysis by examining case-study time-series plots of the variability in more detail within

defined space/time cells, as done in [6]. We separate space and time variability, in both a Eulerian and Lagrangian sense, and for each fixed or drifting cell we estimate standard deviation statistics to gain understanding of the subgrid-scale variability they represent. Then we summarize fluctuation statistics for the entire 4-day period over the large coverage area of a single radar in which the drifters resided. Finally, we offer conclusions and speculation as to what these statistics mean in terms of radar measurements and their short space/time variations.

II. DRIFTER DEPLOYMENT FOR APRIL 1-4, 2008 TESTS

Some 37 drifters were deployed from April 1-4, 2008. As described in [6], when currents are moderate or strong, drifters normally are picked up as they drift outside the desired fixed observation cell and reseeded on the other side continuously. During this period, however, the mean currents were weak over most of the radar observation area. Therefore the drifters were left in the water for the entire period. Fig. 1 shows the trails of the drifters over the entire 4-day period. We also show in the figure two fixed circular cells that will be examined in detail in subsequent sections, as case studies. They were selected to be in a region with a high population of drifters.

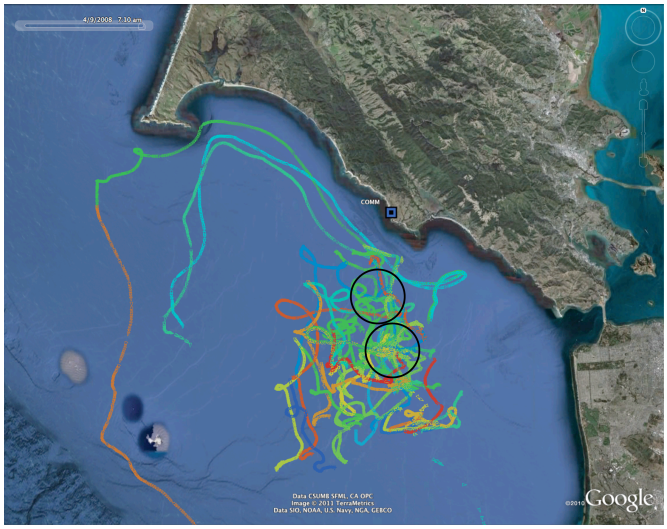

Figure 1. Depiction of drifter deployment area West of Golden Gate, showing COMM SeaSonde site. Tracks of some 37 drifters are shown above over a 4-day period. Two fixed circular areas are indicated that are studied as examples in more detail below.

III. RADAR MEASUREMENTS AND PROCESSING

All radars measure target positions and velocities in a polar coordinate system. Radial velocity obtained from the Doppler shift of the echo from Bragg-resonant waves is the most accurate radar observable. Range to the scattering cell is also an accurate measurement. Bearing or polar angle from any HF radar is the noisiest measurement; radar errors -- whether biases and random fluctuations -- enter via this observable. However, errors in bearing translate to radial velocity errors when the radial estimates are placed on a fixed polar grid. For SeaSonde HF radars, bearing is determined using the MUSIC direction-finding algorithm [8]; at 13 MHz, a polar map of radial velocities is produced every 10 minutes, after averaging approximately 2.5 power cross spectra.

Along with each 10-minute radial velocity map file, uncertainties are produced and included. These are called "spatial uncertainties" because they are the standard deviations of the different radial velocities (due to random fluctuations) falling on the same fixed polar bearing. I.e., they actually were misplaced in bearing from their true positions by the noisiness.

Most SeaSonde users then desire to average these 10-minute radials at each fixed grid point over an hour; this averaging process we have called "merging." In the merging processing, a standard deviation over the 6-7 time samples within that hour is calculated also and outputted within the merged files. This is called the "temporal uncertainty." Both types of uncertainties have been shown to be meaningful for interpretating the noisiness in the radial velocities themselves. In the subsequent analyses, we will work with both the 10-minute radar radial velocities and the hourly merged radial velocities in our studies of surface turbulence.

IV. VELOCITIES IN FIXED EULERIAN CELLS - CASE 1

We focus on two fixed circular cells of 3 km radius, located as shown in Fig. 1 with respect to the radar at COMM. We show in Figs. 2 a time history of all of the radially directed velocities of the drifters that passed through these cells during the four days. Time sampling is every 10 minutes.

For the two circular cells shown whose radial velocities are plotted above in Fig. 2, we calculated the radial velocity standard deviations at each 10-minute interval and averaged these over the 4-day time period. Results are 5.6 cm/s (upper) and 4.5 cm/s (lower); the total number points used in the calculations for these cells are 195 and 253 points, respectively.

Next, we show plots in Fig. 3 for these two fixed circular cells that give the maximum (green), minimum (blue), and standard deviations (yellow) of the drifter measurements vs. time. Also plotted are the radar radial velocities (red) for these same cells. Note that the radar radial velocities always lie between the maximum and minimum drifter velocities within these cells, at every point in time.

In Fig. 4, we show results for the same data sets as Fig. 3, but we average drifter and radar measurements over one hour (the time sampling for Fig. 3 was 10 minutes). This stabilizes/ smoothes the curves, but changes the standard deviation statistics very little from those based on the shorter intervals. Here the hourly standard deviations period are 5.8 cm/s (upper) and 4.8 cm/s (lower); the total number of hourly points used in the calculations for these cells are 54 and 66 points, respectively.

For the two circular cells shown whose radial velocities are plotted above in Fig. 2, we calculated the radial velocity standard deviations at each 10-minute interval and averaged these over the 4-day time period. Results are 5.6 cm/s (upper) and 4.5 cm/s (lower); the total number points used in the calculations for these cells are 195 and 253 points, respectively.

In Figs. 3 and 4 we showed maximum and minimum drifter velocities and their standard deviations vs. time as they passed through the two fixed circular cells. We also showed the radar radials averaged over these circular cells vs. time;

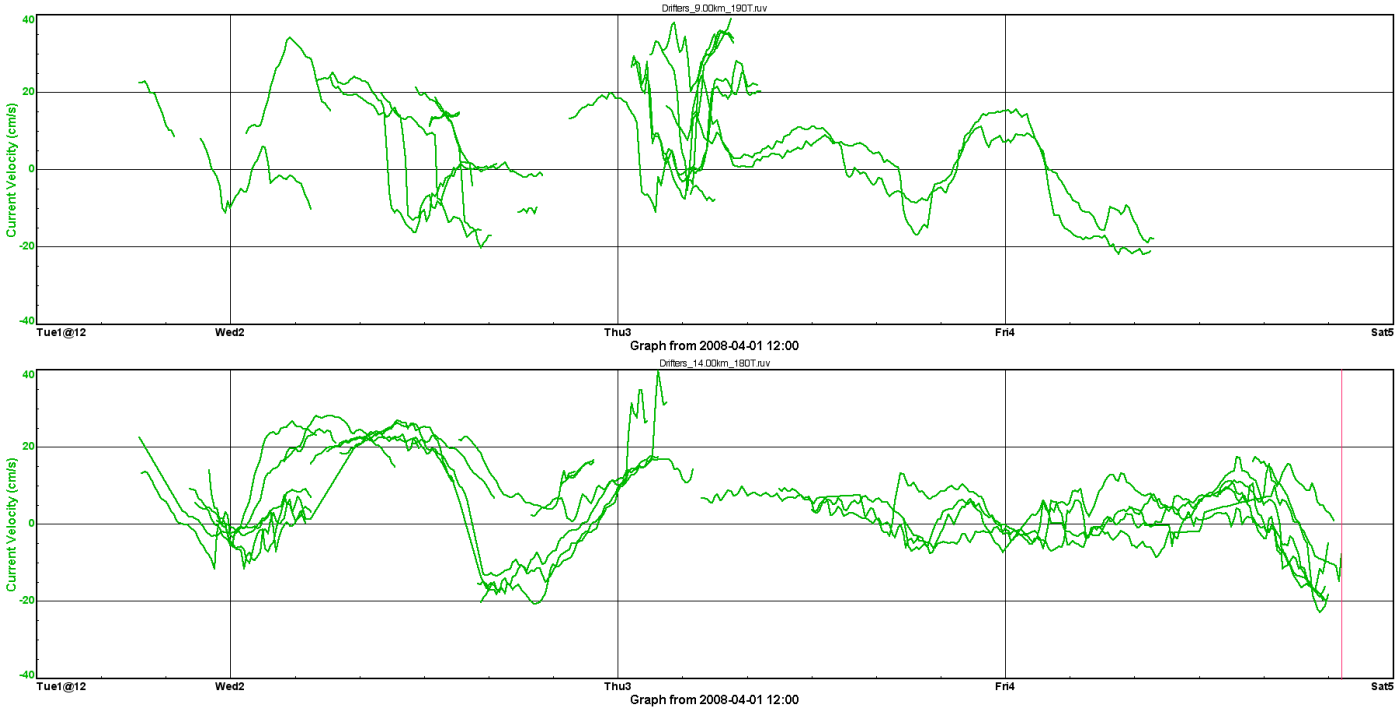

Figure 2. Radial velocities of multiple drifters passing through two fixed 3-km radius circular cells at positions shown in Fig. 1 over four day deployment period. Velocities are sampled every 10 minutes. Upper panel is for Northern circle, lower is for Southern circle of Fig. 1.

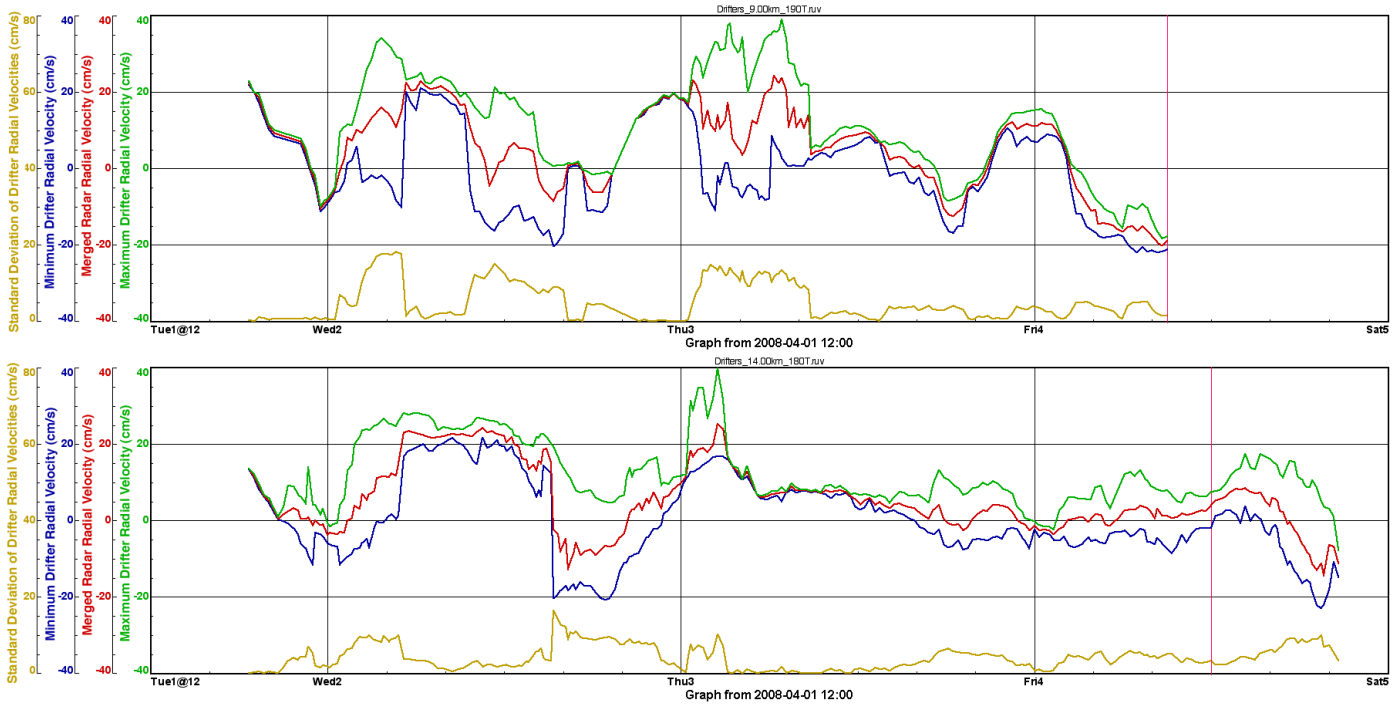

Figure 3. Drifter radial velocity extrema (green and blue) within the cells plotted in Fig. 2. Yellow curve is the standard deviation of all drifter radial velocities within this cell vs. time. Red is the average radar radar velocity at the same times.

this latter curve fell within the maximum and minimum drifter velocities.

Before leaving this section, we examine two measures of standard deviation for the radar velocities -- spatial and

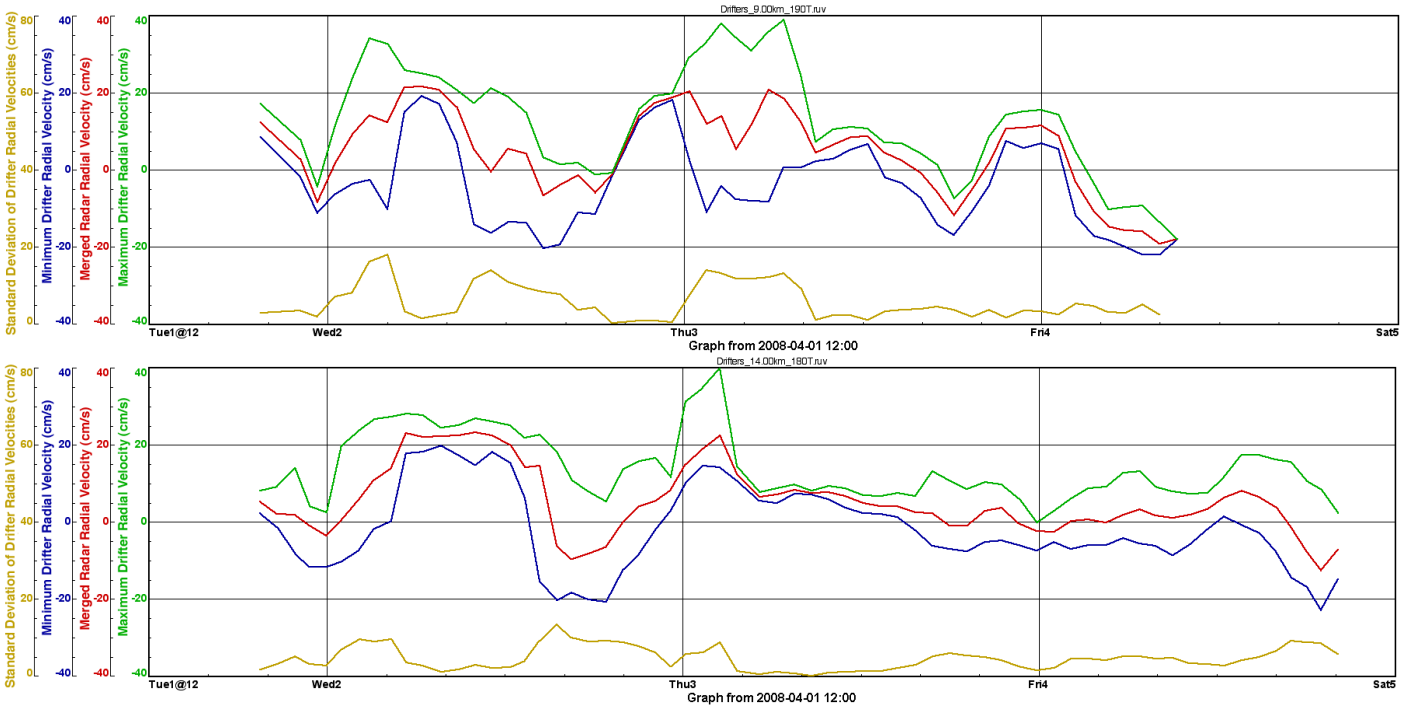

Figure 4. Drifter radial velocity extrema (green and blue) within the cells plotted in Fig. 2, but averaged over one hour rather than 10 minutes as done in Fig. 3.

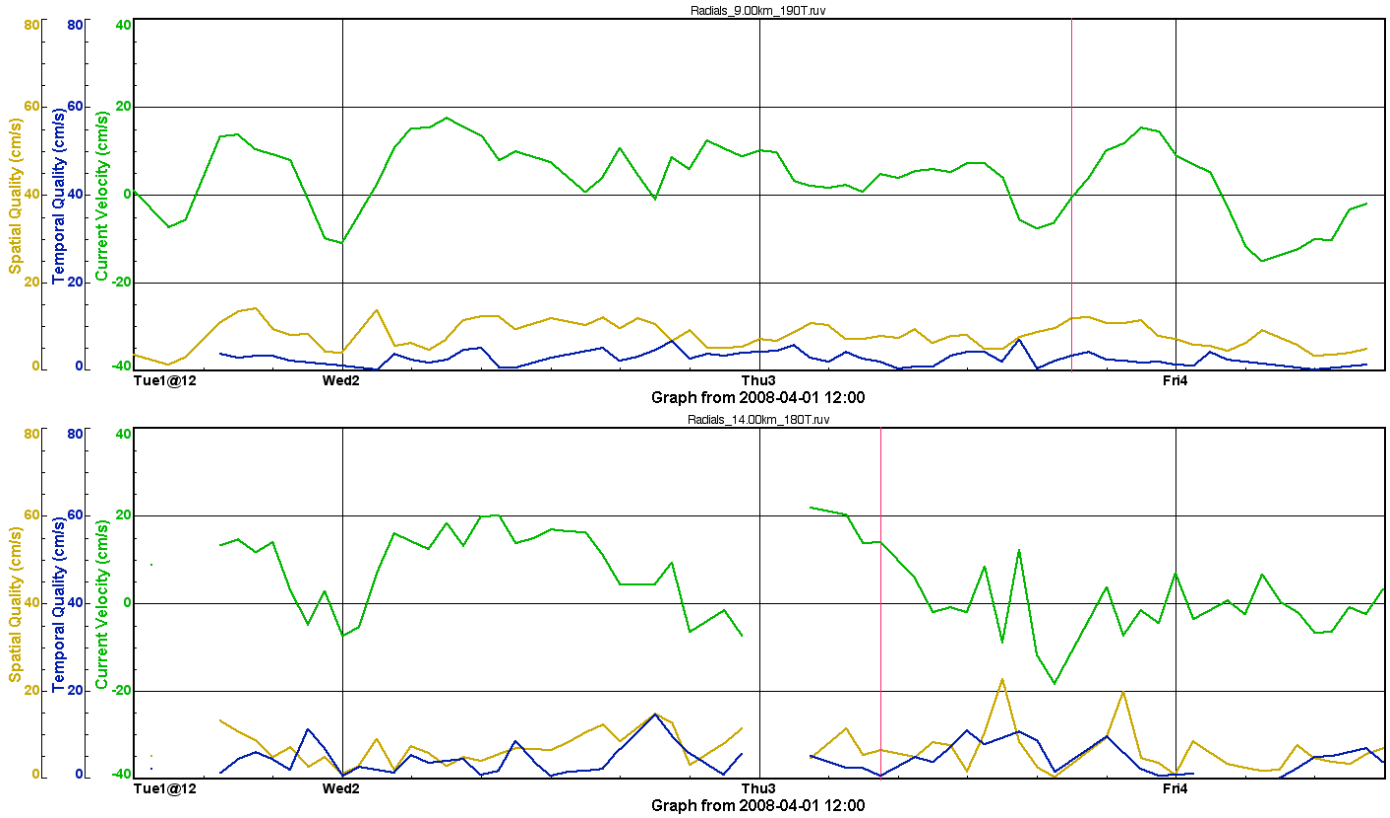

Figure 5. Mean hourly radar radar velocity (green) for the two circular cells being analyzed. Yellow curve is the spatial standard deviation of the radar radial velocity, and blue is its temporal standard deviation, as defined in the text.

temporal -- defined as:

- Spatial Standard Deviation: At each point in time (10-minute intervals) we calculate the standard deviation of the radial velocities that fall on the polar radar grid points encompassed within each of the two circular cells.
- Temporal Standard Deviation: In this we take the mean radial velocity of all of the polar radar grid points encompassed by the two circular cells at each 10-minute time point, and then calculate the standard deviation of these over an hour.

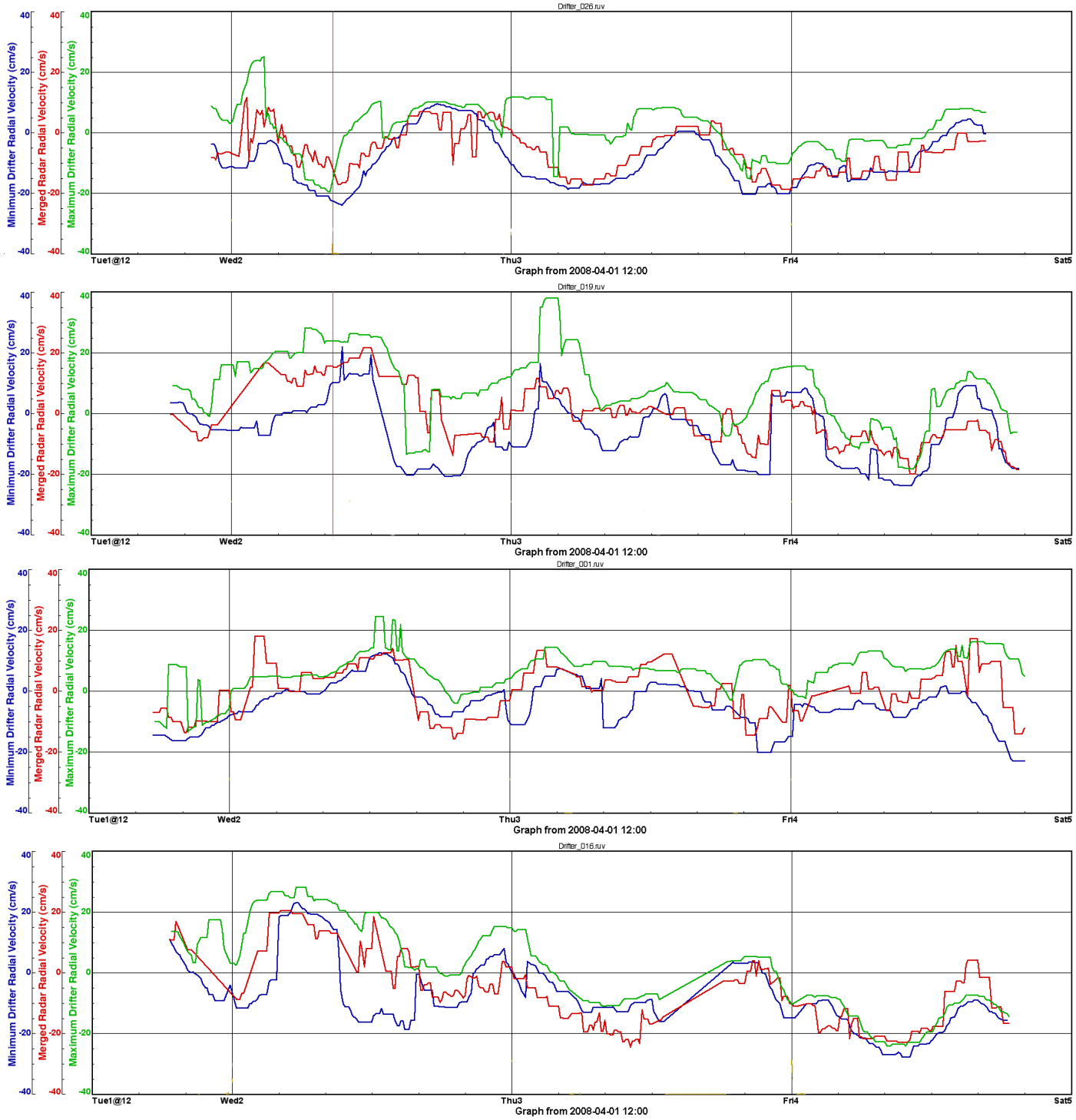

Figure 6. Drifter radial velocity extrema (green and blue) for four circular cells with 3 km radius that are attached to a single drifter and follow it as it moves through the 4-day time span. Each of the panels follows a different drifter. Comparisons are made among all drifters lying within this moving cell. The radar radials (red) are the spatial average within that moving cell. Time averaging and sampling shown is hourly.

We note that these two definitions capture essentially the "spatial quality" and "temporal quality" uncertainties outputted and contained within hourly SeaSonde radial velocity files, except that here they are calculated within circles rather than polar range/bearing cells inherent to radar measurements. The results are plotted vs. time in Fig. 5.

Summary statistics for Fig. 5 over the entire 4-day period are: (1) For Northern circular cell: spatial standard deviation is 7.8 cm/s; temporal standard deviation is 2.8 cm/s. (2) For Southern circular cell: spatial standard deviation is 6.5 cm/s; temporal standard deviation is 4.8 cm/s.

V. Velocities in moving Lagrangian cells - Case 2

As a second case study, we examine radial velocities within a moving 3-km radius cell, whose center is attached to an individual drifter. We do this so that we can track several drifters within this cell as they advect with the overall water circulation over the 4-day period. A fixed cell -- as we used in the preceding study -- would only contain single drifters for a couple hours, and thus we would lose this drifter (and others) as they passed through the circle, while new ones entered. By following the flow, our circular cell includes several additional drifters (besides the one the circle is attached to), as they all follow the general flow pattern while responding to the random diffusive turbulence that gives the tracks the random appearance of Figs. 1 and 2.

Within this moving circular cell, we also examine the radial velocities at all of the radar polar grid points. We average these over the moving 3-km cell and over an hour (a typical, favored radar observation period as mentioned earlier). With SeaSonde processing, we call this temporal averaging of radial velocities within a defined radar cell "merging".

We show in Fig. 6 four examples for moving (Lagrangian) cells. The green curve in each plot is the drifter radial velocity that is the maximum within that cell. The blue curve is the minimum drifter radial velocity within that cell. The red curve is the merged radar radial velocity for that moving cell at hourly intervals.

Here again we show both the maximum and minimum drifter velocities within the moving cell. And we compare these extrema with the merged radial velocity measured by the radar at COMM. As is evident, all of the curves exhibit random fluctuations, as they respond to the spatial and temporal turbulence (or subgrid scale variability) of the surface currents. But the three curves also show that the radar measurements nearly always fall between the maximum and minimum drifter velocities for the same cell. All of them are tracking the longer-term circulation to the West of Golden Gate. As mentioned earlier, during this particular 4-day period, both wind-driven and geostrophic flows were weak, so that the tidal signals are seen to dominate the time series.

For the four drifter-following circles represented by the plots of Fig. 6, the standard deviation statistics for the entire set of hourly samples are:

- Drifter #1 Circle: Drifter standard deviation -- 3.1 cm/s; Radar standard deviation -- 6.1 cm/s.
- Drifter #2 Circle: Drifter standard deviation -- 4.9 cm/s; Radar standard deviation -- 9.0 cm/s.
- Drifter #3 Circle: Drifter standard deviation -- 4.2 cm/s; Radar standard deviation -- 7.7 cm/s.
- Drifter #4 Circle: Drifter standard deviation -- 3.6 cm/s; Radar standard deviation -- 8.3 cm/s.

VI. Summary statistics for entire area / time period

The case studies plotted in the figures were done to give some pictorial insight into the variability of surface water as it transports floating objects. It is also within this uppermost layer that HF radars sense velocity from the backscattered echo Doppler shifts. Relevant standard deviations were given for each of the circles examined in these case studies.

However, the two circular cell examples we considered in Section IV are only a small portion of the total span of drifter and radar observations over this period. We therefore provide here summary standard deviations for all possible 3-km radius circular cells within the radar coverage area that contained more than one drifter (two at least are needed for standard deviations and other statistics). Some overlap of the circles was needed to include all of the area, but this overlap was kept to a minimum.

Both the spatial and temporal standard deviation metrics are given. This is done in order to relate them to the spatial and temporal uncertainties for the radar radial velocity estimates that are outputted within the SeaSonde data files. Also, we give below the RMS difference statistics between the radar and drifter radial components. The numbers given in parentheses are the total number of observations entailed in that statistical computation.

- Drifter Spatial Standard Dev.: 4.1 cm/s (23,588)
- Radar Spatial Standard Dev.: 8.2 cm/s (41,573)
- Radar - Drifter Spatial RMS Diff.: 9.3 cm/s (41,657)
- Drifter Temporal Standard Dev.: 1.2 cm/s (14,251)
- Radar Temporal Standard Dev.: 3.2 cm/s (13,497)
- Radar - Drifter Temp. RMS Diff.: 8.8 cm/s (15,254)

VII. Discussion and summary

A. Turbulence Established by Drifter Studies

The value of multiple simultaneous drifter measurements within radar-sized cells lies in establishing the natural subgrid-scale background variability -- or turbulence level -- of the surface currents. For the region of the Pacific West of Golden Gate, we resolved the velocities of 37 drifters over four days into the component radial to the SeaSonde to the North at COMM (Fig. 1). We then examined their standard deviations in a manner resembling the normal processing done with the radar. First, within individual 3-km radius cells, we calculated the standard deviation of all of the drifter radials at each 10-minute interval, to obtain a value (preceding section) of 4.1 cm/s. Although this was obtained for fixed cells, the number is very similar as we allow the cells to drift, centered on any of several possible drifters.

We also calculated the mean drifter velocity for these cells every 10 minutes, and from this, the standard deviation of these numbers over an hour. Typically six samples were used

in this analysis. This drifter temporal standard deviation was 1.2 cm/s. We do not claim that these standard deviations are representative of all locations or all time periods. Much of this upper-layer current turbulence is induced by wave and wind effects. A similar study is presented inside of San Francisco Bay in a companion paper at this meeting, where the physical processes driving the currents are much different.

B. Radar Measurements and Comparisons with Drifters

Similar to drifter statistics summarized in the preceding section, we examined summary statistics for the radar radials at grid points within the same cells. It should be noted that instantaneous drifter velocities by their nature are Lagrangian measurements while radar measurements are Eulerian, i.e., obtained at fixed polar grid points. Here the standard deviations are larger: 8.2 cm/s for spatial standard deviations every 10 minutes, and 3.2 cm/s when the 10-minute spatial means create a temporal standard deviation over an hour. Both are responding to the natural variability of surface currents. Why then are the radar standard deviations larger? At this point we can speculate that radar measurements include other zero-mean random effects. One is the fact that the sea echo itself from which the currents are extracted is a random variable. Another might be the nature of the difference between the Eulerian and Lagrangian processes inherent in the two.

RMS differences between radar and drifter means were done at both the 10-minute sampling interval, and also after six of these were then averaged over an hour. These numbers are 9.3 cm/s (10-minute spatial averages) and 8.8 cm/s (hourly temporal averages of six spatial means), respectively. The means (biases) were very low, because the standard deviations associated with these two RMS differences are 8.5 cm/s (spatial) and 8.0 cm/s (temporal). Therefore, we see that temporal averaging does little to reduce the radar-observed spatial variability over the 10 minute intervals.

Recall again that the standard deviations we are examining for the radar (and drifters) do not include biases. Biases are means that have been removed from our analyses. One can ask, are the RMS differences with essentially negligible mean biases actually radar errors? Thus far, users of HF radar have not been interested in the random surface variability, but are concerned with circulation phenomena of longer time scales, beginning with tides as the shortest. Therefore, the random variability near 8 cm/s seems to be a limit on individual radar measurements over the space/time scales discussed herein (assuming biases have been removed by proper calibration), and for the Pacific location at which this analysis was done. More studies are recommended, because different upper-layer turbulence conditions might be expected to yield numbers higher or lower than our ~8 cm/s numbers here. Also, different processing and averaging schemes should be investigated to reduce these zero-mean random effects on the radar measurements.

REFERENCES

[1] R. H. Stewart and J. W. Joy, "HF radio measurements of surface currents," 1974 Deep-Sea Res., vol. 21, pp. 1039–1049, 1974.

[2] D. E. Barrick, J. M. Headrick, R. W. Bogle, and D. D. Crombie, "Sea backscatter at HF: Interpretation and utilization of the echo," Proc. IEEE, vol. 62, pp. 673–680, 1974.

[3] D. E. Barrick, M. W. Evans, and B. L. Weber, "Ocean surface currents mapped by radar," Science, vol. 198, pp. 138–144, 1977.

[4] R. D. Chapman, L. K. Shay, H. C. Graber, J. B. Edson, A. Karachintsev, C. L. Trump, and D. B. Ross, "On the accuracy of HF radar surface current measurements: Intercomparison with ship-based sensors," J. Geophys. Res., vol. 102 (C8), pp. 18 737–18 748, 1997.

[5] J. T. Kohut, H. J. Roarty, and S. M. Glenn, "Characterizing observed environmental variability with HF Doppler radar surface current mappers and acoustic Doppler current profilers: Environmental variability in the coastal ocean," IEEE J. Oceanic Engr., vol. 31, pp. 876-884, 2006.

[6] C. Ohlmann, P. White, L. Washburn, E. Terrill, B. Emery, and M. Otero, "Interpretation of coastal HF radar-derived surface currents with high resolution drifter data," J. Atmos. Oceanic Tech., vol. 24, pp. 666 - 680, 2007.

[7] M. Cook, "Preliminary comparisons of HF radar- and drifter-derived surface currents in the Gulf of the Farrallones," ROW8 Workshop, Honolulu, HI, 2008.

[8] D. E. Barrick and B. J. Lipa, "Evolution of bearing determination in HF current mapping radars," Oceanography, vol. 10, pp. 72-75, 1997.